International Journal of Thermophysics, Vol. 4, No. 2, 1983

Pressure Tensor and Viscosity Coefficients of a Soft Sphere Liquid Under Shear

S. Hess[1,2] and H. J. M. Hanley[1]

Received March 14, 1983

General properties and consequences of the distortion of the structure of a simple liquid subjected to a planar shear flow are reported. In particular, the orientational distribution of particles in the first coordination shell around a given particle is analyzed, and the effect of this distribution on the pressure tensor is discussed. The distorted distribution gives rise to a set of non-Newtonian viscosity coefficients reflecting the occurrence of normal pressure differences in the liquid. Numerical values of these viscosities are given for a soft sphere fluid at 7/8 of the freezing density using the technique of nonequilibrium molecular dynamics. A wide range of shear rates is considered and all viscosity coefficients are found to be functions of the shear rate.

KEY WORDS: nonequilibrium molecular dynamics; non-Newtonian effects; radial distribution function; rheological behavior; viscosity.

1. INTRODUCTION

The structure of a liquid, as characterized by the radial distribution function, is distorted out of equilibrium. In fact, the very existence of a potential contribution to the transport coefficients is evidence of the distortion since the coefficients can be expressed as weighted integrals over the difference between the pair correlation function in nonequilibrium and its equivalent equilibrium value [1–3]. But this is a macroscopic argument and until recently was essentially only formal. The situation has changed with the introduction and exploitation of nonequilibrium molecular dynam-

[1] Chemical Engineering Science Division, National Bureau of Standards, Boulder, Colorado 80303, U.S.A.
[2] Permament Address: Institut für Theoretische Physik, University of Erlangen-Nürnberg, D-8520 Erlangen, Federal Republic of Germany.

0195-928X/83/0600-0097$03.00/0

ics [4–9]: computer experiments made it possible to study the basic phenomena occurring in a nonequilibrium process, to test kinetic theory on the microscopic molecular level, and hence to give direct insight into the distorted microscopic structure of a fluid. This last feature is the purpose of this article. We wish to discuss some general properties of the pair correlation function and of the first coordination shell (nearest neighbors) for a liquid subjected to a shear and to present specific results obtained from a computer simulation. Further, some consequences of the distortion of the structure to the pressure tensor are pointed out and corresponding non-Newtonian features of the model fluid are reported. The work follows earlier studies of Hess [10], Hess and Hanley [11], and Evans [12], who emphasized the essential non-Newtonian characteristics of even very simple spherical fluids. In particular, preliminary studies of the distortion of a soft sphere fluid were reported in ref. [11], and this paper is a more detailed and systematic extension.

This article is organized as follows. First, the pair correlation function, $g(\mathbf{r})$, which depends both on the interparticle distance $r = |\mathbf{r}|$ and direction specified by the unit vector $\hat{r} = \mathbf{r}r^{-1}$ in nonequilibrium, is expanded with respect to tensors constructed from the Cartesian components of r. The expansion coefficients, themselves tensors, are functions of r. The scalar and second rank terms are of particular interest, and we will analyze a fluid undergoing planar Couette flow: in this case, three of the five tensorial components suffice to characterize the anisotropy of the radial distribution function. We present results graphically for the functions [and for the scalar, spherical symmetric, part of $g(\mathbf{r})$] based on a simulation of a soft sphere inverse-12 fluid at a state point about 15% less than the freezing density. These results follow and extend our earlier results [11] by illustrating how the functions vary with the imposed shear or strain rate.

Second, the orientational distribution of particles in the first coordination shell is discussed in some detail. This distribution follows by appropriate integration of the radial distribution function over r. In equilibrium, the distribution is, of course, isotropic, i.e., the nearest neighbors of a central reference particle are found with equal probabilities in all directions. But in nonequilibrium this is not so. Given numerical values of the expansion coefficients of $g(\mathbf{r})$, we display distortion patterns as polar-diagram plots.

Third, some consequences of the shear induced distorted structure are indicated, and a set of viscosity coefficients (of which the shear viscosity coefficient is one) is introduced to characterize the rheological behavior of the liquid. The interrelation between the shear induced distortion, non-Newtonian viscosity and the occurrence of normal pressure differences is pointed out.

2. EXPANSION OF THE RADIAL DISTRIBUTION FUNCTION

We consider a simple liquid of spherical particles which can be subjected to a shear [13]. The pair correlation function $g = g(\mathbf{r})$ is a measure of the probability of finding any second particle at position $\mathbf{r}$ when one given particle is at $\mathbf{r} = 0$. At thermal equilibrium, g is the radial distribution function $g_{eq}(r)$, which depends on the distance r but not on the direction of the vector $\mathbf{r}$ (which can be specified by the unit vector $\hat{r}$); however, in nonequilibrium g becomes a function of r and of $\hat{r}$ or, equivalently of r, θ, and ϕ, where θ and ϕ are the polar angles associated with $\mathbf{r}$. This directional dependence can be accounted for explicitly by expanding $g(\mathbf{r})$ with respect to spherical harmonics [12], $y_{lm}(\theta, \phi)$, or, alternatively, with respect to Cartesian irreducible tensors constructed from the components of the unit vector $\hat{r}$. If the particles are identical, $\mathbf{r}$ and $-\mathbf{r}$ are equivalent so only tensors of even rank occur in the expansion.

The expansion for g can be written as

$$g(\mathbf{r}) = g_{sc}(r) + g_{\mu\nu}(r)\hat{r}_\mu * \hat{r}_\nu \cdots \tag{1}$$

The quantity $g_{sc}(r)$ is the scalar or isotropic contribution to $g(\mathbf{r})$. The second term is of critical importance for the viscosity of the system; it is written in Cartesian component notation with the summation convention. The asterisk indicates the symmetric traceless part of a tensor, for example, for vectors $\mathbf{a}$ and $\mathbf{b}$,

$$a_\mu * b_\nu = \tfrac{1}{2}(a_\mu b_\nu + a_\nu b_\mu) - \tfrac{1}{3} a_\lambda b_\lambda \delta_{\mu\nu} \tag{2}$$

where $\delta_{\mu\nu}$ is the unit tensor.

One can interpret the coefficients of the expansion (1) as orientational averages, specifically,

$$\begin{aligned} g_{sc}(r) &= \frac{1}{4\pi} \int g(\mathbf{r})\, d^2 r \\ \frac{2}{15}\, g_{\mu\nu}(r) &= \frac{1}{4\pi} \int \hat{r}_\mu * \hat{r}_\nu g(\mathbf{r})\, d^2 \hat{r} \end{aligned} \tag{3}$$

The quantities depend in general on r and on the strength of the externally imposed disturbance, in our case the shear rate. We note than an expansion of the form of Eq. (1) has been used to treat nonequilibrium phenomena in colloidal solutions, molecular liquids, and liquid crystals, but has only very recently been applied to simple liquids [14–17].

2.1. Special Geometry: Planar Couette Flow

Consider planar Couette flow with the flow velocity **u** parallel to the x axis and the gradient parallel to the y axis. The shear rate $\gamma = du_x/dy$, and the shear rate tensor is

$$\gamma = \begin{bmatrix} 0 & 0 & 0 \\ \gamma & 0 & 0 \\ 0 & 0 & 0 \end{bmatrix} \tag{4}$$

or, in our notation,

$$\gamma_{\mu\nu} = \gamma e_\mu^x * e_\nu^y \tag{5}$$

with a corresponding vorticity ω,

$$\omega_\mu = \tfrac{1}{2}\epsilon_{\mu\nu\lambda}\nabla_\nu v_\lambda \tag{6}$$

In general, the tensor $g_{\mu\nu}$ has five independent components, but only three exist for the special geometry here:

$$g_{\mu\nu} = g_+ e_\mu^x * e_\nu^y + g_- \tfrac{1}{2}(e_\mu^x e_\nu^x - e_\mu^y e_\nu^y) + g_0 e_\mu^z * e_\nu^z \tag{7}$$

where $g_k(r)$, $k \equiv +, -, 0$, are scalar coefficients. In terms of spherical components of the tensor g, $g^{(m)}$, the coefficients g_+ and g_- are the real and imaginary parts of $g^{(\pm 2)}$ in the corresponding spherical harmonic representation: g_0 corresponds to $g^{(0)}$ where the direction of the vorticity is chosen as a reference axis (the z axis here). The $m = \pm 1$ terms, and consequently terms associated with $e_\mu^x * e_\nu^z$ and $e_\mu^y * e_\nu^z$, vanish for this special geometry. This follows from the fact that these terms, in contradistinction to those included in Eq. (7), are not invariant under the symmetry operation $x, y, z \to -x, -y, z$ which leaves the gradient of the flow velocity field invariant.

On inserting Eq. (7) into Eq. (1) one obtains

$$g(\mathbf{r}) = g_{sc} + g_+ \hat{x}\hat{y} + g_-(\tfrac{1}{2})(\hat{x}^2 - \hat{y}^2) + g_0(\hat{z}^2 - \tfrac{1}{3}) + \cdots \tag{8}$$

where $\hat{x} = r^{-1}r_x$, $\hat{y} = r^{-1}r_y$, and $z = r^{-1}r_z$ are the components of vector **r** parallel to the x, y and z coordinate axes, respectively.

Due to Eq. (7), the second relation in Eq. (3) is equivalent to

$$\frac{2}{15} g_k = \frac{1}{4\pi} \int Y_k g(\mathbf{r})\, d^2 r \qquad k \equiv +, -, 0 \tag{9}$$

where

$$Y_+ = 2\hat{x}\hat{y}, \qquad Y_- = \hat{x}^2 - \hat{y}^2, \qquad Y_0 = \tfrac{3}{2}\left(\hat{z}^2 - \tfrac{1}{3}\right)$$

Thus the coefficients g_k are essentially orientational averages of linear combinations of the spherical harmonics Y_{2m} with $m = \pm 2, 0$.

Equation (8) is the basic relation for this and our other studies [11]. It is formally an extension of the traditional ansatz for the pair correlation function for a system under shear [1–3] which truncates the series at g_+. A truncation assumes that g_+ is linear in the shear rate γ, that g_- and g_0 are of higher order in γ and thus effectively vanish, and that the scalar part g_{sc} is independent of γ. The main purpose, however, of our work here and in previous publications is to demonstrate and to try to interpret that g_+ seems to be nonlinear in γ, that g_- and g_0 should not be considered negligibly small, and that g_{sc} deviates from the equilibrium radial distribution function. As has been pointed out [11, 12], the first effect gives rise to a non-Newtonian viscosity, the second to the existence of normal pressure differences [that is, $p_{xx} \neq p_{yy} \neq p_{zz}$, where these are the diagonal components of the pressure tensor], and the third has interesting thermodynamic consequences since g_{sc} can be related to a hydrostatic pressure.

3. COMPUTER PROCEDURE

The technique used here is a variant of shear nonequilibrium molecular dynamics. In this technique, the model system with particles interacting with a designated intermolecular potential, ϕ, is set up for a conventional equilibrium molecular dynamics calculation at constant density $\rho = N/V$, where N is the number of particles and V is the volume, with periodic boundaries: the equations of motion are solved numerically, in our case with a Gear fifth-order predictor correlator technique, for a sufficient number of time steps to verify conservation of energy and to adjust if necessary the time step increment to achieve this. The system at equilibrium is monitored further in a pseudo canonical ensemble by fixing the kinetic temperature to a preassigned value via velocity scaling. The shear rate, γ, is then introduced by adjusting the periodic boundary conditions in the x-y plane as follows: should a particle leave the primary cell by crossing the x or y face at a particular time step Δt, the returned image is repositioned by an increment $\sim \gamma L \Delta t$, where $L = V^{1/3}$. A least squares adjustment is then made to the velocities of all particles in the cell to ensure that the velocity profile is linear to within a statistical uncertainty and that the shear rate tensor matches to within statistical uncertainty the input value. Viscous heat is removed by controlling the kinetic temperature.

The procedure is pragmatic and there are questions on the fundamentals and on the mechanics of solving the equation in nonequilibrium, introducing the shear and scaling the temperature. Nevertheless the results of the technique have received considerable circumstantial support. Variants of the method give consistent answers [4, 8] and, especially, Evans [17] has developed two independent nonequilibrium molecular dynamics algorithms which give results that agree with corresponding results from our technique to within statistical error. Shear viscosities in the limit of zero shear for both the Lennard-Jones [18] and the hard sphere [9] systems have been estimated and compared with the equivalent direct molecular dynamics Green–Kubo calculation, and the comparisons are satisfactory. Further, Evans and Hanley [19, 20] have proposed a heuristic thermodynamics to describe the properties of a system under shear and have introduced consistency checks and criteria which can be verified.

The system under investigation here was a model fluid of 108 spherical particles interacting with the inverse-12 soft sphere potential truncated at $r = 2.5$:

$$\begin{aligned} \phi &= d/r^{12} \qquad r \leqslant 2.5 \\ \phi &= 0 \qquad\quad r > 2.5 \end{aligned} \tag{10}$$

where d is the potential parameter which can be written in terms of the usual energy and length parameters, $d = \epsilon\sigma^{12}$. Soft sphere systems are conveniently studied at a state point X, where

$$X = \rho/(\sqrt{2}\, T^{1/4}) \tag{11}$$

with T, which is not independent, set at 0.25 so that $X \equiv \rho$. All variables can be expressed in terms of d or in terms of ϵ or σ, but we set d equal to one, as usual, and the mass of a particle, m, equal to one. For convenience, Table I lists the conversion of our variables to "real" variables.

Table I. Some Variables Used in the Computer Simulation[a]

Variable	Simulation variable	Real
Length	r^*	$r = r^*(d/kT)^{1/12}$
Time	Δt^*	$\Delta t = \Delta t^*(d/kT)^{1/12}(m/kT)^{1/2}$
Velocity	v^*	$v = v^*(kT/m)^{1/2}$
Shear rate	γ^*	$\gamma = \gamma^*(d/kT)^{-1/12}(kT/m)^{1/2}$
Viscosity	η^*	$\eta = \eta^* m^{1/2}(kT)^{2/3}/d^{1/6}$
Pressure	p^*	$p = p^*(kT)/(d/kT)^{-1/4}$

[a] Denoted (in this table only) with an asterisk, in terms of the potential parameter d of Eq. (10).

Previous results [21] indicated that the effect of shear on the properties of a system depends strongly on the density: the greater the density, the larger the effects. For this reason the calculations reported in ref. [11] were carried out at a density of 0.8 known to be very close to the freezing density. The interpretation of the results, however, was somewhat clouded by the very interesting phenomenon of shear induced melting [19]. Hence we chose a value of $X = 0.7$ for this study to bypass this difficulty.

3.1. Computer Output

The key output from the simulations were as follows: the kinetic temperature, T,

$$T = \frac{1}{3N} \left\langle \sum_{i}^{N} \left[\mathbf{v}_i - \mathbf{u}(\mathbf{r}_i) \right]^2 \right\rangle \tag{12}$$

where $\mathbf{v}_i$ is the velocity of particle i and $\mathbf{u}$ the streaming velocity at position $\mathbf{r}_i$; the energy per particle, E,

$$E = \frac{1}{N} \left\langle \sum_{i}^{N} \frac{1}{2} \left[\mathbf{v}_i - \mathbf{u}(\mathbf{r}_i) \right]^2 + \sum_{i=j} \phi_{ij} \right\rangle \tag{13}$$

where $\phi_{ij} \equiv \phi(\mathbf{R}_{ij})$ with $\mathbf{R}_{ij} = |\mathbf{r}_i - \mathbf{r}_j|$; the elements of the shear rate tensor, Eqs. (4) and (5); and the elements of the pressure tensor $\mathbf{P}$,

$$\mathbf{P} = \frac{1}{V} \left[\sum_{i}^{N} \left[\mathbf{v}_i - \mathbf{u}(\mathbf{r}_i) \right] \left[\mathbf{v}_i - \mathbf{u}(\mathbf{r}_i) \right] + \sum_{i=j} \mathbf{R}_{ij} \frac{\partial \phi_{ij}}{\partial \mathbf{r}_i} \right] \tag{14}$$

The expansion coefficients of Eq. (8) are also evaluated by histograms:

$$\begin{aligned} Fg_{\mathrm{sc}} &= \tfrac{2}{15} \langle N \rangle \\ Fg_{+} &= 2 \langle \hat{x}\hat{y} \rangle \\ Fg_{-} &= \langle \hat{x}^2 - \hat{y}^2 \rangle \\ Fg_{0} &= \tfrac{3}{2} \langle \hat{z}^2 - \tfrac{1}{3} \rangle \end{aligned} \tag{15}$$

where $F = (8/15)\pi r^2 \Delta r \rho$. The angle brackets denote an average for the quantity between r and $r + \Delta r$, a distance r from a given central particle averaged over all particles.

Runs of 50,000–75,000 time steps were made for shear rates in the range $0.05 \leqslant \gamma \leqslant 1.0$. The results are listed in Table II and will be discussed in more detail in Section 5. One notices that the calculated values of the

Table II. Results of the Simulation of the Soft Sphere System at $X = 0.7$ with $T = 0.25$[a]

Shear rate									
Designated	Calc	Temperature	p	$T^{-2/3}\eta_+$		$T^{-2/3}\eta_-$		$T^{-2/3}\eta_0$	
0.05	0.0518	0.2507	2.381	2.345	[2.319]	−0.07	[−0.06]	−0.13	[−.09]
0.08	0.0810	0.2493	2.380	2.153	[2.146]	0.06	[−0]	0.02	[−0]
0.09	0.0904	0.2487	2.383	2.272	[2.243]	0.11	[0.08]	0.01	[−0]
0.10	0.0984	0.2506	2.379	2.351	[2.302]	0.14	[0.11]	0.08	[0.08]
0.12	0.1148	0.2498	2.388	2.303	[2.282]	0.03	[0.04]	0.04	[0.02]
0.13	0.1294	0.2508	2.393	2.132	[2.107]	0	[0.02]	0.08	[0.07]
0.14	0.1398	0.2495	2.390	2.195	[2.137]	0.18	[0.18]	0.11	[0.10]
0.15	0.1540	0.2510	2.390	2.098	[2.064]	0.17	[0.16]	0.14	[0.12]
0.168	0.166	0.2499	2.396	2.289	[b]	0.02	[b]	0.10	[b]
0.20	0.1966	0.2501	2.400	2.188	[2.116]	0.12	[0.10]	0.10	[0.10]
0.3025	0.3040	0.2498	2.4287	2.074	[2.020]	0.09	[0.10]	0.12	[0.10]
0.44	0.4344	0.2505	2.4787	2.013	[1.961]	0.04	[0.05]	0.13	[0.11]
0.50	0.5018	0.2526	2.499	1.954	[b]	0.06	[b]	0.16	[b]
0.7225	0.7246	0.2525	2.578	1.772	[b]	0.05	[b]	0.16	[b]
1.0	0.9990	0.2552	2.710	1.631	[1.581]	0.03	[0.04]	0.19	[0.16]
0	0	0.2501	2.375						

[a] p is the pressure $[\frac{1}{3}\operatorname{tr} P]$ and η_k $(k = +, -, 0)$ are transport coefficients calculated from Eq. (31). Values in brackets were obtained from the alternate Eq. (29). The last entry is for an equilibrium run in the pseudo-canonical ensemble. We have multiplied the transport coefficients by $T^{-2/3}$ (Table I) so the presentation is consistent with our previous work [4, 21].
[b] Integration values unobtainable.

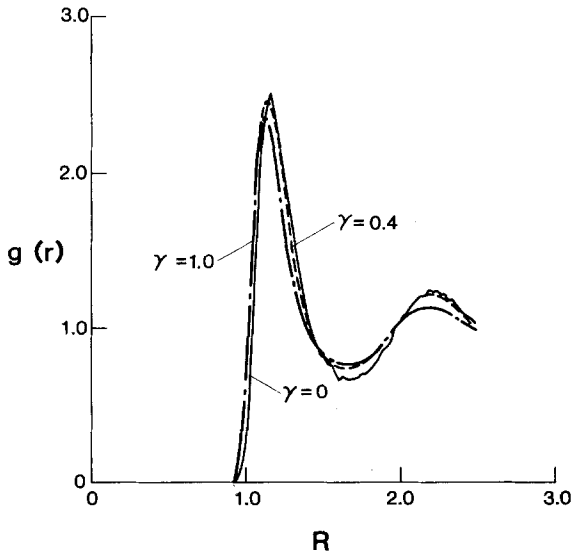

Fig. 1. Plot of the equilibrium radial distribution function (solid curve) compared to the scalar coefficients $g_{sc}(r)$ of Eq. (1) from results for two values of the shear rate, $\gamma = 0.4$ and 1.0.

shear rate are close to the input values, as they should be: similarly the scaled temperature is within 0.5% of the fixed mean value of 0.25 unless the shear rate is high. In this latter case, however, the signal to noise ratio is also high. The histograms of Eq. (15) were constructed for each run giving estimates of the coefficients g_{sc} and g_k. Values for sample shear rates are displayed in Figs. 1 and 2. There are several points here. First, with respect to Fig. 1, the minima and maxima of g_{sc} are less pronounced under shear, as compared with the equilibrium value. Furthermore, there is a shift of the first maximum towards smaller distances. This compression is responsible for the shear enhancement of the (scalar) hydrostatic pressure. Clearly the primarily induced anisotropy described by g_+ is the largest of the second

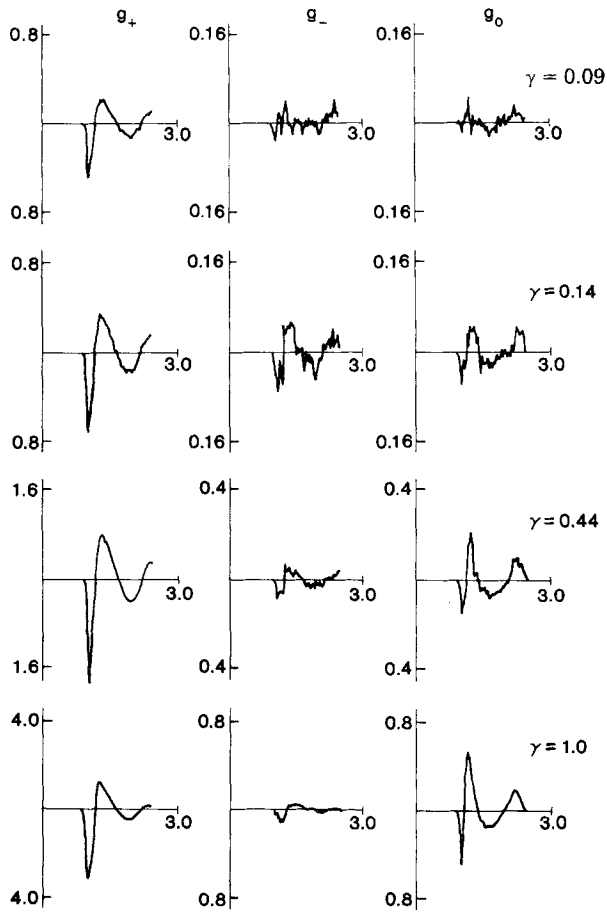

Fig. 2. Plots of the coefficients g_+, g_-, and g_0 of Eq. (9) for four values of the shear rate $\gamma = 0.09$, 0.14, 0.4, and 1.0.

rank tensorial coefficients; the g_- and g_0, however, are definitely nonzero and, as is qualitatively apparent, depend on γ in a nonlinear way. Furthermore, it is interesting that g_0, which is comparable in size with g_- for the smaller shear rates, becomes considerably larger than g_- at higher shear rates. The large g_0 for $\gamma = 1$ is indicative of a kind of uniaxial ordering of the directional correlation between two particles with the symmetry axis parallel to the vorticity (z direction).

4. ORIENTATIONAL DISTRIBUTION OF THE FIRST COORDINATION SHELL

The number of particles found in a sphere of radius R within a solid angle around $\hat{r}$ is

$$\mathcal{N}(\hat{r}, R) = \rho \int_0^R g(\mathbf{r}) r^2 \, dr \tag{16}$$

where $\int g(\mathbf{r}) d^3r = V$ and $\rho = N/V$. If we insert the expansion Eq. (1) into Eq. (16), we have

$$\mathcal{N}(\hat{r}, R) = \frac{1}{4\pi} n(R) + \hat{r}_\mu * \hat{r}_\nu \rho \int_0^R g_{\mu\nu} r^2 \, dr + \cdots \tag{17}$$

where $n(R) = 4\pi\rho \int_0^R g_{sc} r^2 \, dr$. We note that there is an implicit dependence on the shear rate for $\mathcal{N}$ which enters via the values for g. Using the symmetry adapted ansatz (7) for $g_{\mu\nu}$ leads to

$$\mathcal{N}(\hat{r}, R) = \frac{1}{4\pi} \left[n(R) + n_+(R) \hat{x}\hat{y} + n_-(R) \left(\frac{1}{2} \right) (\hat{x}^2 - \hat{y}^2) \right.$$

$$\left. + n_0(R) \left(z^2 - \frac{1}{3} \right) + \cdots \right] \tag{18}$$

where

$$n_k(R) = 4\pi\rho \int_0^R g_k(r) r^2 \, dr \qquad k = 0, +, - \tag{19}$$

Again, $n(R)$ and $n_k(R)$ will be shear-rate dependent and, further, the sign of $n_k(R)$ will depend on the integration limits for g_k: $n_k(R)$ can be either positive or negative as one can see by inspection of Fig. 2.

As in previous work [11], it is often convenient to write Eq. (20) in terms of polar angles of the unit vector $\hat{r}$:

$$4\pi\mathscr{N} = n + \tfrac{1}{2}\sin^2\theta\left[n_+ \sin 2\phi + n_- \cos 2\phi\right] + n_0\left(\cos^2\theta - \tfrac{1}{3}\right) \qquad (20)$$

Equation (20) thus describes the orientation distribution of particles around a reference particle. Here we consider the distribution within the first coordination shell, which one can define as the shell whose radius corresponds to the first minimum in $g_{sc}(r)$, i.e., $R \approx 1.5$.

Equation (20) can be expressed for any set of θ and ϕ of interest. For example, for the plane of the shear, the x-y plane for which $\theta = \pi/2$, the equation becomes

$$4\pi\mathscr{N} = n - \tfrac{1}{3}n_0 + \tfrac{1}{2}\left(n_+ \sin^2\phi + n_- \cos^2\phi\right) \qquad (21)$$

Given, therefore values of g_{sc} and g_k we can construct a polar plot for the variation of $\mathscr{N}$ with ϕ. As an example, Fig. 3 shows the result for the fluid subjected to a shear of one.

If γ was zero, the plot would be, of course, a circle of radius n with the distance from the center to the curve in a specific direction a measure of

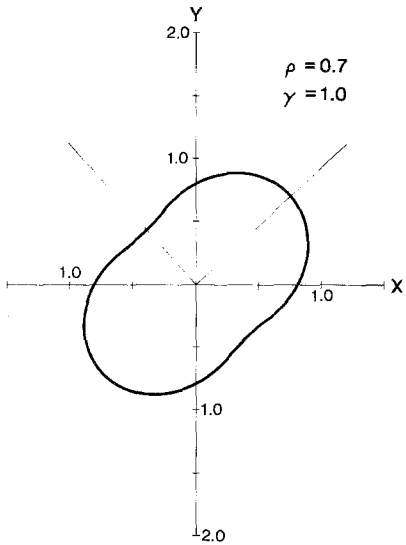

Fig. 3. Plot of the distribution $4\pi\mathscr{N}$ of Eq. (21) for the x-y plane (the plane of the shear) for the fluid subjected to a shear of 1.0. We have subtracted 5.0 from the numerical value of $4\pi\mathscr{N}$ to emphasize the distortion pattern. The principal axis is at $\sim 47°$; the 45°–135° axes are drawn for reference.

the probability of finding a nearest neighbor in that direction. In the lowest order in the shear rate for which $n_+ \sim \gamma$ and $n_0 \approx n_- \approx 0$, one would have an ellipse (provided $n_+ \ll n$) with principal axes in the $\pi/4$, and $3\pi/4$ directions with respect to the x axis. As remarked in the introduction, such a distortion always occurs when a fluid is subjected to a shear and, in fact, the coefficient n_+ is related to the shear viscosity coefficient. If $n_- \neq 0$, the ellipse will be rotated, and the highest probabilities for nearest neighbors will be found at the angles

$$\phi_{\max} = \pi/4 - \chi;\ 5\pi/4 - \chi \tag{22}$$

where

$$\tan 2X = n_-/n_+ \tag{23}$$

[A nonzero n_0 will affect the reference $(n - \frac{1}{3}n_0)$ only.]

Distortion in the x-z or y-z planes can also be illustrated. In this case Eq. (20) reduces to

$$4\pi\mathcal{N} = n \pm \tfrac{1}{2}n_- \sin^2\theta + n_0\left(\cos^2\theta - \tfrac{1}{3}\right) \tag{24}$$

(with the plus sign for the x-z expression). The expression is simple to interpret: if n_- and n_0 are zero, a polar plot will be circular even if $\gamma \neq 0$. Hence any deviation from a circle indicates a nonzero n_- or n_0. The curves for the y-z plane have been drawn as Fig. 4 and such deviations are obvious.

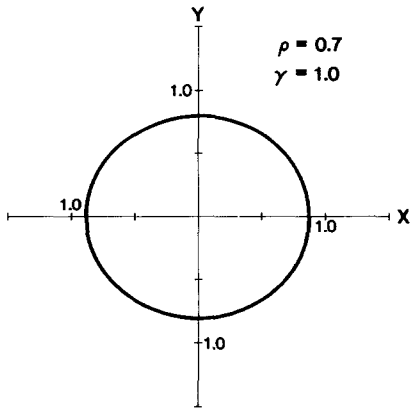

Fig. 4. Plot of the distribution $4\pi\mathcal{N}$ of Eq. (24) for the $y - z$ plane for the fluid under a shear of 1.0. As in Fig. 3, we plot $4\pi\mathcal{N}$ less 5.0. Note the elliptical shape.

We should also remark that the plots are functions of the integration limit R. One could choose a value of R so that the n_k are negative or even zero and the distortion patterns would reflect this. We refer to refs. 11 and 22 for a series of detailed plots.

The distortion curves can be regarded as an instructive interpretation of the basic result that the expansion coefficients g_{sc} and g_k are γ-dependent. On a macroscopic level, these properties are reflected in the pressure tensor and in a rather complex rheological behavior; as will be shown next, the nonlinearity of the distortion of the radial distribution function entails a shear rate dependent viscosity and normal pressure differences.

5. THE PRESSURE TENSOR

One can write the pressure tensor $P_{\mu\nu}$ as the sum of an isotropic scalar part $p\delta_{\mu\nu}$ and a symmetric irreducible traceless part $\overleftrightarrow{p}_{\mu\nu}$, viz.,

$$P_{\mu\nu} = p\delta_{\mu\nu} + \overleftrightarrow{p}_{\mu\nu} \tag{25}$$

where, in terms of the function g,

$$\begin{aligned} p &= -\frac{1}{6}\rho^2 \int d^3r g\, r \frac{\partial \phi}{\partial r} \\ \overleftrightarrow{p}_{\mu\nu} &= -\frac{1}{2}\rho^2 \int d^3r g\, r_\mu \partial_\nu \phi \end{aligned} \tag{26}$$

If the expansion (1) is inserted into Eq. (26) and the integrations over the angles of the unit vector $\hat{r}$ performed, we find

$$\begin{aligned} p &= -\frac{2}{3}\pi\rho^2 \int_0^\infty r^3 g_{sc} \phi'\, dr \\ \overleftrightarrow{p}_{\mu\nu} &= -\frac{4}{15}\pi \int_0^\infty r^3 g_{\mu\nu} \phi'\, dr \end{aligned} \tag{27}$$

where the relation $r_\mu * \partial_\nu = \hat{r}_\mu * \hat{r}_\nu r(d\phi/dr)$ has been used. We next insert the form of $g_{\mu\nu}$ as given by Eq. (7) to obtain

$$p_{\mu\nu} = p_+ 2e_\mu^x * e_\nu^y + p_- (e_\mu^x e_\nu^x - e_\mu^y e_\nu^y) + p_0 2e_\mu^z * e_\nu^z \tag{28}$$

where the coefficients p_k are

$$p_k = -\frac{2\pi}{15}\rho^2 \int_0^\infty r^3 g_k(r) \phi'\, dr \qquad k = +, -, 0 \tag{29}$$

and are related to the Cartesian components of the pressure tensor by

$$p_+ = p_{xy}; \qquad p_- = \tfrac{1}{2}(p_{xx} - p_{yy}); \qquad p_0 = \tfrac{1}{2}\left[p_{zz} - \tfrac{1}{2}(p_{xx} + p_{yy})\right] \quad (30)$$

Equation (30) allows viscosity coefficients to be introduced by

$$p_k = -\eta_k \gamma \qquad k = +, -, 0 \quad (31)$$

where $\gamma = \partial u_x/\partial y$ as before; η_+ is the shear viscosity and in general depends on γ; and η_- and η_0 are associated with normal pressure differences (i.e., that $p_{xx} \neq p_{yy} \neq p_{zz}$) and they too depend on γ.

As an aside we remark that the coefficients η_- and η_0 are identified with the viscometric function ψ_1 and ψ_2 defined, for example, in ref. 23:

$$p_{xx} - p_{yy} = -\psi_1 \gamma^2$$

$$p_{yy} - p_{zz} = -\psi_2 \gamma^2 \quad (32)$$

Hence

$$\psi_1 \gamma = 2\eta_-; \qquad \psi_2 \gamma = -(2\eta_0 + \eta_-) \quad (33)$$

We prefer to consider the set η_+, η_-, and η_0 rather than the perhaps more familiar set η_+, ψ_1, and ψ_2 for two reasons. First, the η_k are related to the spherical components of $\eta^{(m)}$ of the viscosity tensor (with the direction of the vorticity, the z axis, as the reference axis) in a simple manner [24]: η_+ and η_- are essentially the real and imaginary parts, respectively, of $\eta^{(\pm 2)}$, while η_0 corresponds to $m = 0$. Second, a theoretical analysis shows [10] that different theoretical mechanisms lead to $\eta_- \neq 0$ and $\eta_0 \neq 0$: more specifically, the rotation induced by the vorticity $\hat{\omega}$ of the flow field gives rise to $\eta_- \neq 0$, and $\eta_0 \neq 0$ is generated by terms of even power in the symmetric traceless shear rate tensor $\gamma_{\mu\nu}$.

A fourth viscosity coefficient, η', could also be introduced because not only are $p_{xx} \neq p_{yy} \neq p_{zz}$ in general for a fluid under shear, but the average, expressed as $\frac{1}{3}$ of the trace of P, is not the same as the equilibrium hydrostatic pressure, p_{eq}. We see this, for example in Fig. 1 since g(equil) $\neq g_{sc}$; see Eq. (24). Hence

$$p_{eq} - p = -\eta' \gamma \quad (34)$$

5.1. Results from the Simulation

Table I gives values for p, η_+, η_-, and η_0 for the soft sphere system. Given are values estimated directly from the elements of the pressure tensor

via Eq. (14) and, for η_+, η_-, and η_0, values obtained by integration of Eq. (29) to $r = 2.5$ using the results for the expansion coefficients via the histograms of Eq. (15). It should be recalled that the expressions of Eq. (29) are for the potential contribution only, whereas the results from the pressure tensor contain a kinetic contribution. We would, therefore, expect the results from Eq. (29) to be lower, as is the case. We do not know, however, the density dependence of $\eta_{+,-,0}$ (kinetic) (for their shear rate dependence, see ref. 25); such a dependence nevertheless is expected to be very small.

Comments are as follows. First, we have reported a quantitative estimation from microscopic arguments of the normal pressure difference coefficients η_- and η_0 for a wide range of shear rates. Second, since η_- and η_0 are generally positive except at low shear where, presumably, they are effectively zero, tensor element $p_{yy} > p_{xx}$ and $(p_{xx} + p_{yy})/2 > p_{zz}$. (It should be pointed out that whereas η_+ must be positive, η_- and η_0 can, in principle, be positive or negative.) Curves for η_- and η_0 are plotted in Fig. 7. Qualitatively, the behavior of η_- and η_0 agrees with the theoretical calculations [10] based on the Kirkwood-Smoluchowski equation. Third, we plot Δp versus $\gamma^{3/2}$, where $\Delta p = p(\gamma) - p$ $(\gamma = 0)$, and η_+ versus $\gamma^{1/2}$ as Figs. 5 and 6. Similar γ-dependences were found for the Lennard-Jones fluid, the m-6-8 fluid [26], and our preliminary results for soft spheres [21].

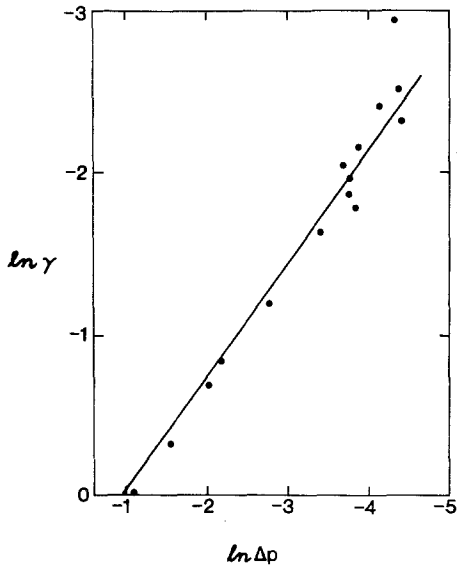

Fig. 5. Variation of pressure ($\frac{1}{3}$ tr **P**) with the shear rate. We have plotted $\ln \Delta p$ versus $\ln \gamma$.

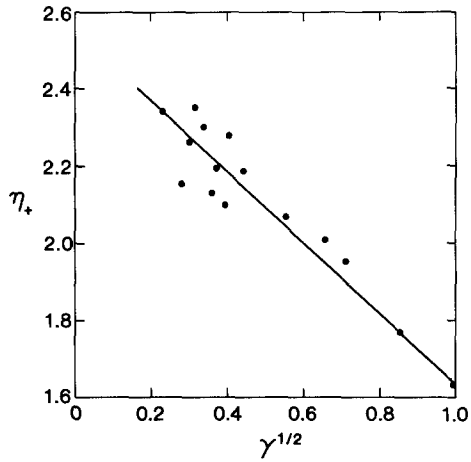

Fig. 6. Variation of the viscosity η_+ with the square root of the shear rate.

Fourth, it can easily be shown from the integration of Eq. (29) to the first coordination shell gives a viscosity coefficient limit which is very close to the asymptotic or macroscopic value. In other words, the pressure tensor, and consequently the viscosity coefficients, reflect directly the distortion of the first coordination shell.

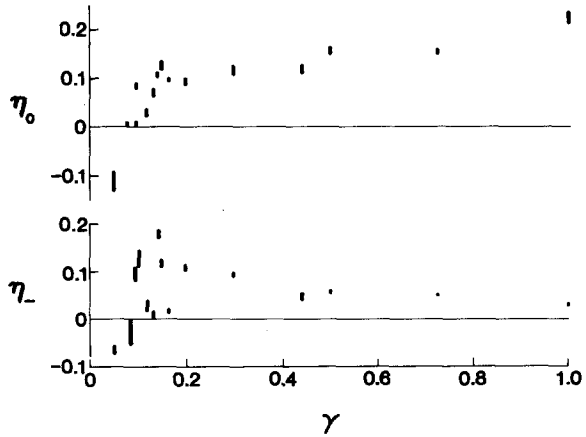

Fig. 7. Variation of the viscosity coefficients η_- (lower curve) and η_0 (upper curve) with shear rate. The size of the points is a reflection of the error of that result.

6. CONCLUSIONS

We have discussed some general properties of the distortion of the structure of a simple liquid subjected to a plane shear flow. In particular we have looked at the pair correlation function: given this, one can study the distribution of particles around a central particle or, alternatively, examine the pressure tensor from a microscopic viewpoint. A set of viscosity coefficients η_+, η_-, and η_0 (of which the shear viscosity η_+ is one element) can be defined to characterize the pressure tensor: η_- and η_0 can be identified with normal pressure differences, i.e., that $p_{xx} \neq p_{yy} \neq p_{zz}$.

Earlier work [11] was extended, and we obtained results for a soft sphere liquid at 7/8 of its freezing density using the technique of nonequilibrium molecular dynamics. The variation of the viscosity coefficients η_- and η_0 with shear rate has been presented but the results should be regarded as preliminary since we need more data for a range of densities and for other model systems before one can arrive at a quantitative conclusion on their behavior. The effect of system size should also be studied. The observation that (1) η_- and η_0 can be nonzero and (2) that all coefficients η_+, η_-, and η_0 are functions of the shear rate is interesting. It suggests a reassessment of the nature of nonlinear or "rheological" behavior in fluids. Such behavior is traditionally associated only with fluids of complex structure. While some authors have argued this is not necessarily so, and that one should consider the shear dependent behavior of all fluids with respect to an appropriate time scale, the computer calculations give concrete evidence. In this context, the experiments of Clark and Ackerson should be mentioned [27]. These authors have investigated shear induced distortion using light scattering techniques in colloidal suspensions. The parallels with the computer simulations are very strong [28].

Along these lines a simple argument can be made to equate non-Newtonian behavior of simple and of nonsimple liquids. On the microscopic level, the basic mechanism associated with shear flow is a deformation and a rotation of the orientational distribution of particles caused by the shear rate tensor and the vorticity, respectively. For nonspherical (stiff) particles and polymer (loose) molecules, the orientation of the axis of the molecules or of the links between polymer beads [29] is affected by the shear; whereas for simple liquids, the shear affects the direction of the vector joining neighboring particles. In this sense, therefore, nonlinear phenomena in simple liquids is to be expected. Conversely, one can argue that a detailed investigation of the shear rate dependence of the pressure tensor and viscosity coefficients of simple liquids could also provide new insight into the rheology of nonsimple liquids.

ACKNOWLEDGMENTS

This work was supported by the Office of Standard Reference Data with computer funds provided in part by the University of Colorado. We are grateful for helpful discussions with D. J. Evans, who has contributed substantially to many areas of nonequilibrium molecular dynamics. We would also like to thank Karen Bowie for typing the paper.

REFERENCES

1. J. G. Kirkwood, *J. Chem. Phys.* **14**:180 (1946); J. H. Irving and J. G. Kirkwood, *J. Chem. Phys.* **18**:817 (1950).
2. R. Eisenschitz, *Statistical Theory of Irreversible Pressures* (Oxford Univ. Press, Oxford, 1958).
3. H. S. Green, *Handb. d. physik* **10**:1 (1960).
4. W. G. Hoover and W. T. Ashurst, *Theor. Chem. Adv. Perspect.* **1**:1 (1975).
5. T. Naitoh and S. Ono, *J. Chem. Phys.* **70**:4515 (1979).
6. D. J. Evans, *Phys. Rev.* **A22**:229 (1979).
7. D. J. Evans and H. J. M. Hanley, *Physica* **103A**:343 (1980).
8. D. M. Heyes, J. J. Kim, C. J. Montrose, and T. A. Litowitz, *J. Chem. Phys.* **73**:3987 (1980).
9. W. W. Wood and J. Erpenbeck, *J. Stat. Phys.* **24**:455 (1981).
10. S. Hess, *Phys. Rev.* **A22**:2844 (1980); *Phys. Rev.* **A25**:614 (1982).
11. S. Hess and H. J. M. Hanley, *Phys. Rev.* **A25**:1801 (1982).
12. D. J. Evans, *Phys. Rev.* **A23**:1988 (1981).
13. We use the notation of Hess; ref. 10.
14. S. Hess, *Physica* **74**:277 (1974); **86A**:383 (1977).
15. S. Hess, *Z. Naturforsch.* **31a**:1034 (1976).
16. I. Pardowitz and S. Hess, *Physica* **100A**:540 (1980).
17. D. J. Evans, *Physica* **118A**:51 (1983).
18. B. E. Holian and D. J. Evans, *J. Chem. Phys.* **78**:5147 (1983).
19. H. J. M. Hanley and D. J. Evans, *J. Chem. Phys.* **76**:3225 (1982).
20. D. J. Evans and H. J. M. Hanley, *Phys. Lett.* **80A**:175 (1980).
21. D. J. Evans and H. J. M. Hanley, *Phys. Lett.* **79A**:178 (1980).
22. H. J. M. Hanley, D. J. Evans, and S. Hess, *J. Chem. Phys.* (in press).
23. R. B. Bird, R. C. Armstrong, and O. Hassager, *Dynamics of Polymeric Liquids, Vol. 1, Fluid Mechanics*, (Wiley, New York, 1977).
24. S. Hess and L. Waldmann, *Z. Naturforsch.* **26A**:1057 (1971); S. Hess, *Physica* **87A**:273 (1977).
25. N. Herdegen and S. Hess, *Physica* **115A**:281 (1982).
26. H. J. M. Hanley and D. J. Evans, *Physica* **103A**:343 (1980).
27. N. A. Clark and B. J. Ackerson, *Phys. Rev. Lett* **44**:1005 (1981).
28. S. Hess, *Phys. Rev.* **A22**:2844 (1980).
29. R. B. Bird, O. Hassager, R. C. Armstrong, and C. F. Curtiss, *Dynamics of Polymeric Liquids, Vol. 2, Kinetic Theory*, (Wiley, New York, 1977).